Bloch Domain Walls in Type-II Optical Parametric Oscillators

Gonzalo Izús and Maxi San Miguel

Instituto Mediterráneo de Estudios Avanzados, IMEDEA (CSIC-UIB),*

E-07071 Palma de Mallorca, Spain

Marco Santagiustina

Istituto Nazionale di Fisica della Materia, Dipartimento di Elettronica e Informatica,

Università di Padova, via Gradenigo 6/a, 35131 Padova, Italy

Abstract

Evidence of Bloch domain walls in nonlinear optical systems is given. They are found in the transverse field of optical parametric oscillators, when the polarization degree of freedom and the cavity birefringence and/or dichroism are taken into account. These domain walls arise spontaneously and present defects where Bloch walls of different chirality join. Two dynamical regimes are found: in a first one the vector field approaches a final homogeneous state, while in another one the walls are continuously generated and annihilated. This dynamical behaviour is caused by the fact that walls of different chirality move spontaneously with opposite velocities.

The search of novel transverse structures in nonlinear optical systems is actively pursued[1], because of their possible application in all-optical signal processing and because they are clear examples of pattern formation in systems away from equilibrium[2]. These structures are the result of the interaction of nonlinearity and diffraction in transverse, spatially extended devices such as nonlinear cavities of large Fresnel number. Among the nonlinear systems analyzed, the optical parametric oscillators (OPO's) have received a very large attention from the theoretical viewpoint, demonstrating the possible formation of patterns[3], domain walls[4−6] and localized structures[7−9]. Very recently, patterns were finally found in an experimental realization of a continuous-wave triply resonant OPO[10].

A particularly interesting class of structures that have been investigated in the context of optics is that of domain walls, i.e. fronts connecting two different solutions. Ising walls are fronts for which the field vanishes at the core of the wall. They have been predicted for type-I, degenerate OPO's (DOPO's)[4,5,7], as well as for other optical systems[11−14] closely related to the OPO's. These Ising walls connect two solutions for which the complex amplitude of the electric field has the same modulus but opposite phase. The reported experimental observation of walls separating different solutions in parametric mixing[15] and the generality of such front solutions in nonlinear optics[16] justify the interest of an extented study of the existence and stability of domain walls in OPO's. The stability of Ising walls has been recently debated; though the intrinsic stability of such fronts has been demonstrated[17], their observation beyond the initial transient requires the presence of walk-off[6] or vortex dynamics[18].

Besides Ising walls, another kind of front structures, i.e. Bloch walls, have been investigated in systems described by a complex order parameter satisfying an evolution equation with a broken phase invariance[19–22]. Bloch walls differ from Ising walls because the field amplitude does not vanish at the core of the wall. Far from the Ising-Bloch transition the amplitude of a Bloch wall is nearly constant, while the phase rotates in passing from one domain to the other. In this Letter we demonstrate that Bloch walls can also be formed in OPO's when cavity birefringence and/or dichroism are accounted for.

The OPO we consider consists of a ring cavity filled with a birefringent, nonlinear quadratic medium and pumped by a uniform, external laser beam at frequency 2ω. Weak birefringence and dichroism, that take into account the small imperfections of the cavity, are also included in the model; for the sake of simplicity we suppose that only one mirror is birefringent and dichroic. Note that the mirror principal axes (i.e. those along which the Jones matrix, representing the polarization transformation, is diagonal) can be rotated with respect to the principal axes of the crystal (i.e. those along which the susceptibility matrix is diagonal) by an angle ϕ. In the mean field approximation and considering the paraxial and the single longitudinal mode approximations for all the fields, the equations describing the time evolution for the linear polarization components of the second harmonic ($B_{x,y}(x,y,t)$) (SH) and the first harmonic ($A_{x,y}(x,y,t)$) (FH) electric fields (where A_x, B_x are ordinary polarized beams and A_y, B_y are extraordinary polarized[23]), in a type-II, phase-matched OPO are:

$$\partial_t B_x = \gamma'_x[-(1+i\Delta'_x)B_x + ia'_x\nabla^2 B_x + c'_x B_y + 2iK_0 A_x A_y + E_0] \tag{1}$$

$$\partial_t B_y = \gamma'_y[-(1+i\Delta'_y)B_y + ia'_y\nabla^2 B_y + c'_y B_x] \tag{2}$$

$$\partial_t A_x = \gamma_x[-(1+i\Delta_x)A_x + ia_x\nabla^2 A_x + iK_0 A_y^* B_x + c_x A_y] \tag{3}$$

$$\partial_t A_y = \gamma_y[-(1+i\Delta_y)A_y + ia_y\nabla^2 A_y + iK_0 A_x^* B_x + c_y A_x] \tag{4}$$

The coefficients $\gamma_{x,y}, \gamma'_{x,y}$ (cavity decay rates), $\Delta_{x,y}, \Delta'_{x,y}$ (cavity detunings) and $a_{x,y}, a'_{x,y}$

(diffraction coefficients) are defined as in refs.[3,23]; due to the birefringence of the nonlinear crystal and the dichroism of the cavity they can be all slightly different, even when the signal and idler are frequency degenerated. Other parameters are the nonlinearity K_0 and the injected pump E_0 that, for the sake of simplicity, we considered to be linearly polarized in the same direction of the phase-matched component of the second harmonic B_x. Hence, the highly mismatch component B_y neither is pumped nor is nonlinearly coupled with other components; under these conditions we found that B_y does not influence the dynamics although it is linearly coupled to B_x through c'_y. The linear coupling coefficients $c_{x,y}, c'_{x,y}$ are related to the dichroism, the birefringence and the relative inclination between the crystal and the mirror axes (ϕ) by:

$$c_{x,y} = \frac{p + i\delta}{T \pm p\,cos(2\phi)} sin(2\phi), \;\; c'_{x,y} = \frac{p' + i\delta'}{T' \pm p' cos(2\phi)} sin(2\phi) \tag{5}$$

where the plus (minus) sign applies for the x (y) polarized component. The mirror dichroism $2p$ ($2p'$) is the ratio between the difference of reflectivities and the average reflectivity of the FH (SH) polarization components; the mirror birefringence 2δ ($2\delta'$) is the ratio between the differential phase delay and the average delay of the FH (SH) polarization components. Finally T (T') is the average transmittivity for the FH (SH). A linear coupling between A_x and A_y was also taken into consideration in previous studies of type-II OPO's showing phase-locking effects[24,25]. That term accounted for the insertion of intracavity wave-plates (quarter-wave or half-wave) in an OPO with no transverse spatial dependence. The equations we have introduced include previous results as special cases and hence they are a more general representation of the effects of the cavity birefringence and dichroism.

A linear stability analysis shows that the trivial solution $A_{x,y} = 0$, $B_x = (1 + i\Delta'_y)E_0/(1 -$

$\Delta'_x\Delta'_y - c'_x c'_y + i(\Delta'_x + \Delta'_y))$, $B_y = c'_y E_0/(1 - \Delta'_x\Delta'_y - c'_x c'_y + i(\Delta'_x + \Delta'_y))$, is stable for $E_0 < E_c$ where $E_c = (1 + i\Delta_x)\sqrt{1+\tilde{\Delta}^2}$, $\tilde{\Delta} = (\gamma_x\Delta_x + \gamma_y\Delta_y)/(\gamma_x + \gamma_y) > 0$ if $c_{x,y} = c'_{x,y} = 0$. No analytical solution could be found for $c_{x,y}, c'_{x,y} \neq 0$, but E_c could be determined through numerical solutions; we note that the threshold decreases as the coupling strengths $|c_{x,y}|, |c'_{x,y}|$ increase. This analysis means that, for a homogeneous external pump of weak intensity, the OPO presents a transversally uniform stationary state for the field at frequency 2ω: no signal or idler are generated.

If the pump amplitude exceeds E_c, the steady state becomes unstable and the signal and idler fields are generated. For $\tilde{\Delta} > 0$ homogeneous perturbations have the largest growth rate. In this case two homogeneous solutions $A^+_{x,y}$ and $A^-_{x,y}$ of equal amplitude and phase-shifted by π radiants ($A^+_{x,y} = -A^-_{x,y}$) bifurcate from $A_x = A_y = 0$. They are equivalent solutions, having the same probability to be selected starting from random initial conditions close to the unstable state. For a spatially extended system, the formation of phase domains where the field is equal to one or the other solution can be expected. For a type-II OPO we demonstrate that Bloch walls can form, being the linear coupling $c_{x,y}$ the parameters that break the phase invariance and control the transition from Bloch to Ising walls. Note that this transition has been demonstrated for a parametrically forced complex Ginzburg-Landau equation (PCGLE)[19,20] being the forcing amplitude the tuning parameter. Such equation, in the non-variational case, is related to the model of a singly resonant, degenerate OPO[26] (SRDOPO), but with a main difference, which actually prevents the observation of Bloch walls in SRDOPO's. In fact, the formation of Bloch walls in a PCGLE requires the parametric forcing amplitude to be smaller than one third of the (positive) linear term[19]; however, to guarantee signal generation the parametric forcing in the SRDOPO must be larger than the linear loss (negative) term.

Numerical integrations of eqs.(1) confirm that stationary uniform domains, where $A_{x,y}$ are either $A^+_{x,y}$ and $A^-_{x,y}$, form spontaneously: for small values of $c_{x,y}, c'_{x,y}$ separating fronts are of the Bloch type while for larger values they are of the Ising type. For these simulations -in 2D-, the real and imaginary parts of the trivial unstable solution for both the FH and the SH fields were randomly perturbed with a real Gaussian white noise (delta-correlated in space and time) to obtain the initial condition.

In Fig.1 an example of a one-dimensional (1D) Bloch wall for A_x is shown. The phase can rotate in two possible senses across the interface, clockwise or counterclockwise in the complex plane. In the context of domain walls this characteristic is called the chirality and the interface shown in fig. 1 has positive chirality (clockwise rotation). The wall for A_y has the opposite chirality.

In two dimensions (2D) the domain walls that grow from random initial conditions around the trivial unstable solution can emerge with opposite chirality in different spatial regions. The change of chirality takes place in singular points, where the phase field is not defined and the amplitude is zero (defects). An example of the transient transverse patterns for the component A_x, obtained in 2D, is shown in fig. 2. Observe, in fig. 2a, the interfaces that separate A^+_x from A^-_x (the homogeneous regions); walls of different chirality are represented respectively by the black or white curves ($B_\pm$). Defects associated with the changes of chirality are observed as black dots in the intensity field (fig. 2b) while the phase field is shown in fig. 2c. Similar structures have been reported in the description of the ordering process of a nonconserved anisotropic XY-spin system in 2D[27].

The dynamics of Bloch walls in 2D can be of two types, depending on the detuning and damping values, and it is influenced by the curvature of the walls themselves. For $\gamma_x\Delta_x = \gamma_y\Delta_y$ flat Bloch walls are stable (this can be checked by observing that 1D walls do not move for the same parameters); then, the ordering process is mainly controlled by the curvature of the fronts. This leads to the growth of a phase at the expenses of the other and the annihililation of all the defects. This behavior is similar to the dynamics of the 2D, PCGLE in the variational case[27]. For $\gamma_x\Delta_x \neq \gamma_y\Delta_y$ walls of different chirality move in opposite directions in a 1D system. Then, in 2D, the defects are notably stable and the Bloch walls of different chirality tend to spiral around them[20]. The fronts of equal chirality annihilate, when they collide, and new ones are generated by the defects; this results in a persistent, spatio-temporal, complex behaviour, as seen in fig 3. In this figure, the formation of Bloch walls generated by an ordered set of defects is shown.

The coupling coefficients $c_{x,y}, c'_{x,y}$ control the wall width and the transition from Bloch to Ising type. In particular the wall width diverges to infinity as $c_{x,y} \to 0$ and Bloch walls are not stable for $c_{x,y} = 0$. In fact, when the birefringent and dichroic coupling are removed phase invariance is restored into eqs. (1). However, note that even a small amount of birefringence or dichroism is sufficient to make these structures stable and therefore they are likely to be observed in Type-II OPO's, due to any weak imperfection of the cavity. For $c_{x,y} = 0$ Ising wall are not stable either; however, they become stable for larger values of $|c_{x,y}|$, for which Bloch walls loose their stability. In this regime spontaneous Ising wall formation occurs. Beyond the Bloch-Ising transition labyrinthine patterns are formed[14,15]. This phenomenon can be associated with the fact that, for large $|c_{x,y}|$, flat Ising walls are "modulationally unstable", like those predicted for second harmonic generation[11], i.e. tend to increase their curvature.

In conclusion we have demonstrated that Bloch walls can be found as transverse pattens of nonlinear optical systems, in particular in type-II optical parametric oscillators. They appear when there exists a small linear coupling between the signal and the idler that stems from the birefringence and/or dichroism of the cavity mirrors. Two dimensional Bloch walls are characterized by sections of different chirality, separated by phase defects where the field amplitude is zero. Two dynamical regimes, that depend on the decay rates and the detunings, are found: in the first one, the wall dynamics is dominated by the curvature and a final homogeneous state is reached; in a second regime, the walls spiral around the stable defects and a persistent creation and annihilation of fronts is observed. The transition from Bloch to Ising walls have been observed when the linear coupling strength is increased.

This work was supported by the European Commission project QSTRUCT (FMRX-CT96-0077) and by DGICYT (Spain), project PB94-1167. The authors acknowledge very clarifying discussions with G-L Oppo. M.S. also acknowledges fruitful discussions with L. Palmieri.

REFERENCES

*. http://www.imedea.uib.es/PhysDept.

1. Special issue of Jour. of Opt. B: Quant. Semiclass. Opt., **1**, (1999).

2. M.C. Cross, P.C. Hohenberg, Rev. Mod. Phys. **65**, 851 (1993).

3. G-L Oppo, M.Brambilla, L. A. Lugiato, Phys. Rev. A **49**, 2028 (1994).

4. S. Trillo, M. Haelterman, A. Sheppard, Opt. Lett. **22**, 970 (1997).

5. S. Longhi, Phys. Scr. **56**, 611 (1997).

6. M. Santagiustina, P. Colet, M. San Miguel, D. Walgaef, Opt. Lett. **23**, 1167 (1998).

7. K. Staliunas, V. Sánchez-Morcillo, Phys. Rev. A **57**, 1454 (1998).

8. G.L. Oppo, A.J. Scroggie, W.J. Firth, Jour. Opt. B: Quant. Semiclass. Opt., **1**, 133 (1999).

9. M. Le Berre, D. Leduc, E. Ressayre and A. Tallet, J. Opt. B: *Quant. Semiclass.* Opt. **1**, 153 (1999).

10. M. Vaupel, A. Matre, C. Fabre, Phys. Rev. Lett. **83**, 5278 (1999).

11. U. Peschel, D. Michaelis, C. Etrich, F. Lederer, Phys. Rev. E **58**, R2745 (1998).

12. M. Tlidi, P. Mandel, R. Lefever, Phys. Rev. Lett. **81**, 979 (1998).

13. K. Staliunas, V. Sánchez-Morcillo, Phys. Lett. A **241**, 28 (1998).

14. R. Gallego, M. San Miguel, R. Toral, Phys. Rev. E **61**, 2241 (2000).

15. V. Taranenko, K. Staliunas, C. Weiss, Phys. Rev. Lett. **81**, 2236 (1998).

16. N.N. Rozanov, Progress in Optics, E. Wolf Ed. **35**, 1 (1996).

17. N. Kutz, T. Ernaux, S. Trillo, M. Haelterman, Journ. Opt. Soc. Am B **16**, 1936 (1999).

18. G-L. Oppo, A.J. Scroggie, W.J. Firth, EQEC Digest, (Glasgow, UK) 245 (1998).

19. P. Coullet, J. Lega, B. Houchmanzadeh, J. Lajzerowicz, Phys. Rev. Lett. **56**, 1352 (1990).

20. T. Frisch, S. Rica, P. Coullet, J.M. Gilli, Phys. Rev. Lett. **72**, 1471 (1994).

21. S. Longhi, Europhys. Lett. **37**, 257 (1997).

22. I. P. Arjona, F. Silva, V. Sanchez-Morcillo, E. Roldan and S. G. Valcárcel, unpublished.

23. G. Izús, M. Santagiustina, M. San Miguel, P. Colet, J. Opt. Soc. Am. B **16**, 1592 (1999).

24. H.J. Kimble, Quantum fluctuations in quantum optics-squeezing and related phenomena, (J. Dalibard, J.M. Raimond, J. Zinn-Justin eds.), Elsevier Science Publishers, (1992).

25. D. Lee, N. Wong, Appl. Phys. B **66**, 133 (1998); E.J. Mason, N.C. Wong, Opt. Lett. **23**, 1733 (1998); C. Fabre, E. Mason, N. Wong, Opt. Comm. **170**, 299 (1999).

26. S. Longhi, Jour. Mod. Opt. **43**, 1089 (1996).

27. H. Tutu, Phys. Rev. E **56**, 5036 (1997).

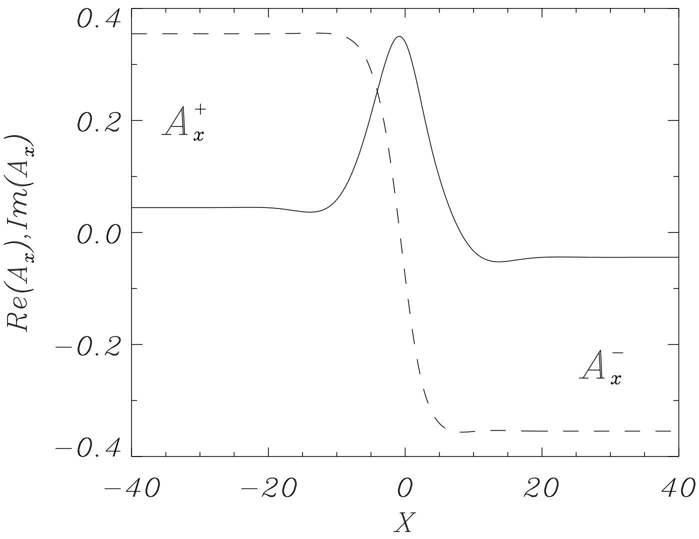
0.4
0.2
0.0
−0.2
−0.4
$Re(A_x), Im(A_x)$
A_x^+
A_x^-
−40
−20
0
20
40
X

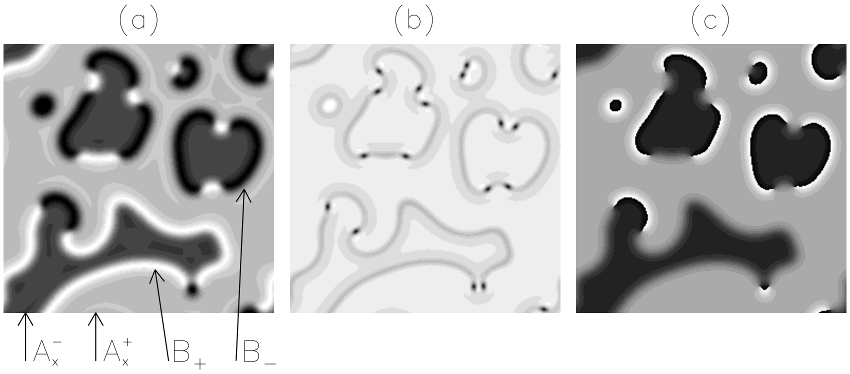

(a)
(b)
(c)
A_x^-
A_x^+
B_+
B_-

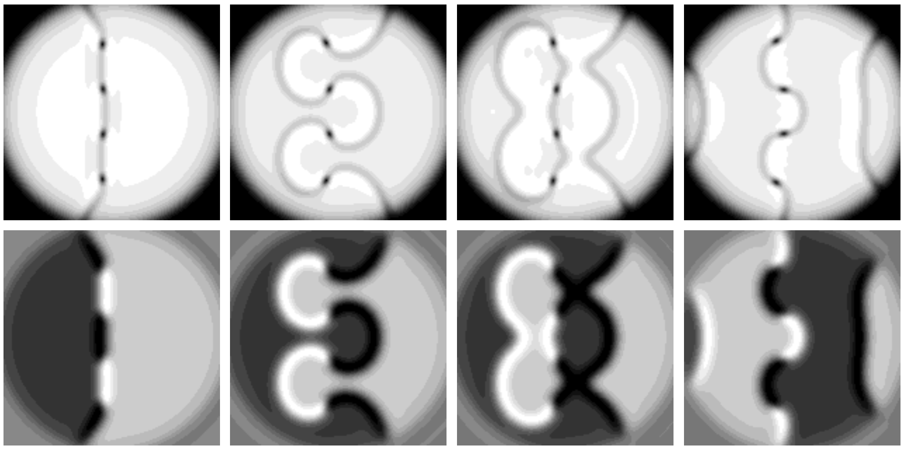

(a) (b) (c) (d)

Figure Captions:

Figure 1: A numerical solution of eqs. (1), in one spatial dimension, showing a Bloch wall. Solid line represents the real part of A_x and the dotted line is the imaginary part. The parameters are $\gamma_x = \gamma'_x = 1$, $\gamma_y = \gamma'_y = 1.002$, $\Delta'_x = \Delta'_y = 0$, $\Delta_x = 0.01$, $\Delta_y = 0.03$, $a'_x = a'_y = 0.125$, $a_x = a_y = 0.25$, $K_0 = 1$, $E_0 = 1.25$, $c'_{x,y} = 0.025(1 - i/2)$ and $c_{x,y} = 0.02i$. $A_x^{\pm}$ indicate the two possible homogeneous stable states.

Figure 2: A snapshot at time t=1600 of the field $A_x(x, y, t)$: respectively a) real part; b) intensity and c) phase. The parameters are $\gamma'_x = \gamma_y = 1$, $\gamma'_y = \gamma_x = 1.002$, $\Delta'_x = \Delta'_y = 0$, $\Delta_x = 0.01$, $\Delta_y = 0.03$, $E_0 = 1.25$, $a'_x = a'_y = 0.125$, $a_x = a_y = 0.25$, $K_0 = 1$, $c'_{x,y} = 0.025(1 + i/2)$ and $c_{x,y} = 0.02(1 + i)$. In fig.(a) we label the different homogeneous stable states $A_x^{\pm}$ and the fronts $B_{\pm}$, which correspond to Bloch walls with positive/negative chirality.

Figure 3: Time evolution of Bloch walls; the intensity (real part) of A_x is shown above (below) for: a) t=0; b) t=1000; c) t=1150; d) t=1550; The parameters are: $\gamma'_x = \gamma_y = 1$, $\gamma'_y = \gamma_x = 1.002$, $\Delta'_x = \Delta'_y = 0$, $\Delta_x = 0.01$, $\Delta_y = 0.03$, $E_0 = 1.25$, $a'_x = a'_y = 0.125$, $a_x = a_y = 0.25$, $K_0 = 1$, $c'_{x,y} = 0.01$ and $c_{x,y} = 0.025$.